Published OnlineFirst March 31, 2011; DOI: 10.1158/0008-5472.CAN-10-2221

Oncogene-Mediated Human Lung Epithelial Cell Transformation Produces Adenocarcinoma Phenotypes *In Vivo*

Ken Sasai[1], Taiko Sukezane[1], Emmy Yanagita[2], Harumi Nakagawa[1], Azusa Hotta[1], Tomoo Itoh[2], and Tsuyoshi Akagi[1]

Abstract

It has been challenging to engineer lung adenocarcinoma models via oncogene-mediated transformation of primary cultured normal human cells. Although viral oncoprotein-mediated malignant transformation has been reported, xenografts derived from such transformed cells generally represent poorly differentiated cancers. Here, we demonstrate that the combined expression of multiple cellular factors induces malignant transformation in normal human lung epithelial cells. Although a combination of four genetic alterations, including hTERT overexpression, inactivation of the pRB and p53 pathways, and KRAS activation, is insufficient for normal human small airway epithelial cells to be fully transformed, expression of one additional oncogene induces malignant transformation. Notably, we have succeeded in reproducing human lung adenocarcinoma phenotypes in the flanks of nude mice by introducing an active form of PIK3CA, CYCLIN-D1, or a dominant-negative form of LKB1 in combination with the four genetic alterations above. Besides differentiated lung cancer, poorly differentiated cancer models can also be engineered by employing c-MYC as one of the genetic elements, indicating that histologic features and degree of differentiation of xenografts are controllable to some extent by changing the combination of genetic elements introduced. This is the first study reporting malignant transformation of normal lung epithelial cells in the absence of viral oncoproteins. We propose that our model system would be useful to identify the minimal and most crucial set of changes required for lung tumorigenesis, and that it would provide a broadly applicable approach for discovering attractive therapeutic targets. *Cancer Res; 71(7); 2541–9.* ©*2011 AACR.*

Introduction

More than 1 million people worldwide die from lung cancer each year, making it the leading cause of cancer mortality in both women and men. Non–small-cell lung cancer, accounting for approximately 80% of all lung cancer cases with adenocarcinoma being the major subtype, is often diagnosed at an advanced stage and has a poor prognosis despite advances in early detection and standard treatment (1, 2). The treatment and prevention of lung cancer are major unmet needs that can be improved by a better understanding of the molecular basis and evolution of the disease. Identifying the minimal and most crucial set of changes required for tumorigenesis is vital in developing the best targets for early detection and therapeutic intervention. To address this issue, *in vitro* model systems using genetically manipulated normal human cells have been developed (3, 4).

Several groups have attempted to render human lung epithelial cells immortalized and transformed (5–7). In these studies, 3 of the genetic alterations that occur in a majority of human non–small-cell lung cancers are induced by retroviral-mediated gene transfer: introduction of *hTERT* (telomerase catalytic subunit) and inactivation of the pRB- and p53-pathways. This seems to be a reasonable strategy, as telomerase is almost universally expressed at high levels in lung cancers (8), the loss of p53 function is observed in approximately 50% of non–small-cell lung cancers, and loss of p16 protein expression caused by promoter methylation or homozygous deletion inactivates the pRB pathway in approximately 70% of non–small-cell lung cancers (1, 2). Lundberg and colleagues have succeeded in the malignant transformation of primary human airway epithelial cells using the SV40 early region as one of the genetic elements (7). It is widely acknowledged that SV40 large T antigen inactivates 2 major tumor suppressors, p53 and pRB, through direct binding (9). However, this viral oncoprotein also possesses multiple uncharacterized functions (10), which makes it difficult to estimate the importance of additional genetic alterations in epithelial cells immortalized by the SV40

Authors' Affiliations: [1]KAN Research Institute, Inc., and [2]Division of Diagnostic Pathology, Kobe University Hospital, Kobe, Japan

Note: Supplementary data for this article are available at Cancer Research Online (http://cancerres.aacrjournals.org/).

Corresponding Author: Tsuyoshi Akagi, KAN Research Institute Inc., 6-7-3 Minatojima-Minamimachi, Chuo-ku, Kobe 650-0047, Japan. Phone: 81-78-306-5910; Fax: 81-78-306-5920. E-mail: t-akagi@kan.eisai.co.jp

doi: 10.1158/0008-5472.CAN-10-2221

Published OnlineFirst March 31, 2011; DOI: 10.1158/0008-5472.CAN-10-2221

early region. Because a combined alteration of 4 cellular elements has failed to convert normal human bronchial epithelial cells into tumorigenic cells (5), one of the greatest challenges facing the field is to engineer transformed lung epithelial cells by the expression of a set of cellular factors.

In the present study, we have succeeded in transforming normal human small airway epithelial cells (HSAEC) without the expression of viral oncoproteins. Interestingly, the tumors' histological features represent well-differentiated or poorly differentiated human lung cancers depending on the combination of genetic elements introduced. Our model system provides a powerful new approach to assess the contribution of individual genetic alterations in lung cancer development.

Materials and Methods

Cell culture and soft-agar colony formation assay

Normal HSAECs established from a 19-year-old Caucasian female and from a 47-year-old Hispanic male (HSAEC-2) were purchased from Lonza. They were cultured on collagen-coated dishes in a serum-free SAGM medium supplemented with various growth factors supplied by the manufacturer (SAGM Bullet Kit; Lonza). The soft-agar colony formation assay was done as described previously (11), using Dulbecco's modified Eagle's medium instead of SAGM medium, and senescence-associated β-galactosidase (SA-β-gal) staining was carried out using the Senescence β-Galactosidase Staining Kit (Cell Signaling Technology). In all cases (both adherent culture and soft-agar assay), cells were maintained at 37°C under a low oxygen environment (3% O_2 and 5% CO_2) in a humidified incubator.

Retroviral vectors and retroviral-mediated gene transfer

All retroviral vector plasmids used in this study are listed in Supplementary Table S1, and maps for the plasmids expressing different levels of an activated form of KRAS ($KRAS^{V12}$) are shown in Supplementary Figure S1A. Retroviral-mediated gene transfer was carried out as described previously (11) using the retrovirus-packaging constructs (pGP, pE-Ampho, pE-Eco) obtained from Takara Bio. The murine ecotropic retrovirus receptor (*Eco* VR) was first introduced into HSAECs by using amphotropic virus to make human cells susceptible to the subsequent infection with ecotropic viral vectors. The *Eco* VR-expressing HSAECs were then infected with retroviruses expressing CDK4, hTERT, and a dominant-negative form of p53 (p53CT, c-terminal region of wild-type p53; see also Supplementary Fig. S1B), and infected cell populations were selected in culture media containing blasticidin (2 μg/mL), G418 (500 μg/mL), and L-histidinol (4 mmol/L) to obtain immortalized HSAECs (hereafter termed 4T53 cells). As shown in Supplementary Figure S2, the 4T53 cells remained diploid. One or more oncogenes were further introduced into the 4T53 cells, and infected cell populations were selected in culture media containing puromycin (1 μg/mL) and/or bleocine (40 μg/mL) for 2 weeks. In all cases, cultures arose from the polyclonal expansion of infected cells, and all resultant cells were used at population doublings of less than 15.

Xenograft propagation experiment

All mouse studies were carried out according to protocols approved by the institutional Animal Care and Use Committee at KAN Research Institute, Inc. Single cell suspensions of 1×10^6 HSAECs were resuspended in 50% Matrigel (BD Bioscience) and injected subcutaneously in the flank of 6- to 7-week-old female athymic nude mice (BALB/c *nu/nu*; Japan SLC). Tumor sizes were measured using calipers and tumor volumes were calculated according to the following formula, $ab^2/2$ (*a*, width; *b*, length). Portions of the xenografts were fixed in 10% formalin for histologic analyses, and the remainder were used for primary culture by making a single-cell suspension as described previously (12). The cultures were maintained for 10 days under regular conditions for HSAEC culture as described previously, and were then subjected to biochemical analyses.

Histologic analysis and immunohistochemistry

Formalin-fixed, paraffin-embedded xenograft tissues were sectioned and stained with hematoxylin and eosin (H&E) and alcian blue using standard protocols. Immunohistochemistry was carried out as described previously (13) using the antibodies listed in Supplementary Table S2.

Immunoblotting

Protein determination, SDS-PAGE, and immunoblotting were carried out as described previously (14), and the reactive protein signals were visualized by chemiluminescence using the SuperSignal WestFemto reagent (Pierce). Antibodies used in this experiment are listed in Supplementary Table S2.

Results

HASECs expressing hTERT, CDK4, and a dominant-negative form of p53 (4T53 cells) were immortalized but not transformed (see Table 1), consistent with the previous observation that the combination of 3 genetic alterations, including bypass of the pRB and p53-pathways and overexpression of telomerase, was still not sufficient for malignant transformation of normal human bronchial epithelial cells (5, 6). To inactivate the p53 pathway, we introduced a dominant-negative form of the *p53* gene (p53CT; c-terminal region of wild-type p53, see also Supplementary Table S1), which resulted in the accumulation of the inactivated p53 protein in immortalized HSAECs (Fig. 1A and Supplementary Fig. S1B), as was reported in the previous studies (15–17). As *KRAS* mutations are detected in approximately 20% of non–small-cell lung carcinomas (1, 2), an activated-form of KRAS ($KRAS^{V12}$) was expressed in the 4T53 cells (4T53R cells; Fig. 1A). We found that transduction of high-level of $KRAS^{V12}$ into 4T53 cells resulted in growth arrest with vacuolation (Fig. 1B). As only a small number of cells were positive for SA-β-gal staining (Fig. 1B), the growth arrest observed in the 4T53R (high level) cells might be due to the mechanisms other than oncogene-induced senescence. In contrast, the 4T53R cells with the reduced levels of $KRAS^{V12}$ expression, made by using a different type of expression vector (Supplementary Fig. S1A), did not show any signs of

Published OnlineFirst March 31, 2011; DOI: 10.1158/0008-5472.CAN-10-2221

Table 1. Summary of xenograft propagation experiments

Cell types	Incidence	Latency[a]	Diagnosis	AE1/AE3	VIMENTIN	p63	TTF1
4T53	0/2	N/A	N/A	N/A	N/A	N/A	N/A
4T53M	0/ 4	N/A	N/A	N/A	N/A	N/A	N/A
4T53R	0/6[b]	N/A	N/A	N/A	N/A	N/A	N/A
4T53RM	3/8	58	Poorly differentiated cancer	+	++	−	−
4T53RMB	8/10	51	Poorly differentiated cancer	+	++	−	−
4T53RP	5/5	14	Adenosquamous carcinoma	++	+	+	+
4T53RD	6/6	16	Adenocarcinoma	++	+	+	+
4T53RL	5/6	23	Adenocarcinoma	++	+	+	+

NOTE: Immortalized HSAECs (4T53 cells) infected with retroviral vectors expressing c-MYC (M), $KRAS^{V12}$ (R), BCL2 (B), $PIK3CA^{H1047R}$ (P), CYCLIN-D1 (D) and/or $LKB1^{D194A}$ (L) were injected s.c. into nude mice (1×10^6 cells/site), and mice were observed up to 10 weeks. Tumor incidence, latency, and diagnosis are listed with the results of immunohistochemistry. Immunostaining of AE1/AE3, VIMENTIN, p63, and TTF1 were evaluated by the 3-tiered grading system (++, strongly positive; +, partially positive; −, negative). N/A, not applicable.

[a]Median time (d) for s.c. xenograft to reach 250 mm^3.

[b]Only one case developed very small adenocarcinoma-like tumor (xenograft reached ~140 mm^3 at d 70).

growth arrest (Fig. 1B). We therefore used 4T53R cells with the reduced levels of $KRAS^{V12}$ for further study: levels of KRAS protein were only 2 to 3 times higher in *KRAS*-expressing HSAECs (4T53R, 4T53RM, and 4T53RMB cells) compared with immortalized HSAECs (Fig. 1A).

While the 4T53R cells often failed to form colonies in soft agar (Fig. 1C) or tumors *in vivo* (Table 1), 1 xenograft developed a very small tumor (Table 1) that contained small areas displaying adenocarcinoma-like phenotypes (Supplementary Fig. S3A). However, the tumor comprised mainly of mouse stromal cells (Supplementary Fig. S3A), which might be one of the reasons for its less progressive phenotype. Furthermore, although we attempted to increase tumor incidence by implanting 2×10^6 cells (2-fold higher than in regular conditions), the 4T53R cells failed to form tumors in the flank of nude mice (incidence, 0/4; data not shown). Therefore, we concluded that $KRAS^{V12}$ alone was insufficient for immortalized lung epithelial cells to be fully transformed, which supports the results from a previous study (5). Because *MYC* amplification was detected in 5% to 20% of non–small-cell lung carcinomas (1, 2), we introduced c-MYC into immortalized cells. Although the 4T53 cells expressing c-MYC (4T53M cells) failed to form colonies in soft agar or tumors *in vivo*, the 4T53 cells expressing both $KRAS^{V12}$ and c-Myc (4T53RM cells) grew in soft-agar and propagated in xenografts (Fig. 1C and Table 1).

Although the combined expression of c-MYC and $KRAS^{V12}$ was sufficient for immortalized HSAECs to be transformed, the oncogenic potential of the 4T53RM cells was low: tumor incidence of flank xenograft was only 38% (Table 1) and the tumor took an average of 8 weeks to reach a volume of 250 mm^3. As the 4T53RM cells exhibited several features of apoptosis in adherent culture (data not shown), *BCL2* was additionally introduced into the 4T53RM cells (4T53RMB cells). BCL2 is known to suppress MYC-induced apoptosis, and its expression is associated with 25% to 30% of squamous cell carcinomas and approximately 10% of adenocarcinomas (1). Although only a limited increase in colony number was observed in the 4T53RMB cells compared with the 4T53RM cells (Fig. 1C), the tumor incidence was dramatically increased (80%; Table 1), suggesting that BCL2 suppresses MYC-induced apoptosis and increases tumor formation in transformed HSAECs, as observed with transformed ovarian surface epithelial cells (18).

Histological examination demonstrated that flank xenografts derived from 4T53RM and 4T53RMB cells were comprised mainly of poorly differentiated cancer cells (Fig. 1D). Tumor cells were strongly positive for VIMENTIN and weakly positive for cytokeratins (AE1/AE3, Fig. 1D; CK8/18, data not shown). Interestingly, only one of the 4T53RMB xenografts contained both poorly differentiated and adenocarcinoma-like cancer cells within the same specimen (Supplementary Fig. S3B). However, the majority of the 4T53RMB xenografts did not demonstrate any characteristics of squamous-cell carcinomas or adenocarcinomas, and therefore, we consider that it is difficult to generate differentiated lung cancer models by using this combination of oncogenes. It is possible that the generation of a differentiated cancer might be hampered by the use of c-MYC because it is generally acknowledged that MYC inhibits terminal differentiation of multiple cell types (19). In fact, xenografts derived from c-MYC-transduced human keratinocytes also produced poorly differentiated tumors (20), and overexpression of c-MYC was reported to correlate with poorly differentiated human carcinomas compared with the well and moderately differentiated lung cancers (21). It is also possible that the combination of introduced oncogenes might not recapitulate the genetic alterations of corresponding human lung cancers. Although KRAS, c-MYC, and BCL2 are individually associated with non–small-cell lung cancer, it is unclear whether these genetic alterations occur simultaneously in the same lung cancer patients.

Published OnlineFirst March 31, 2011; DOI: 10.1158/0008-5472.CAN-10-2221

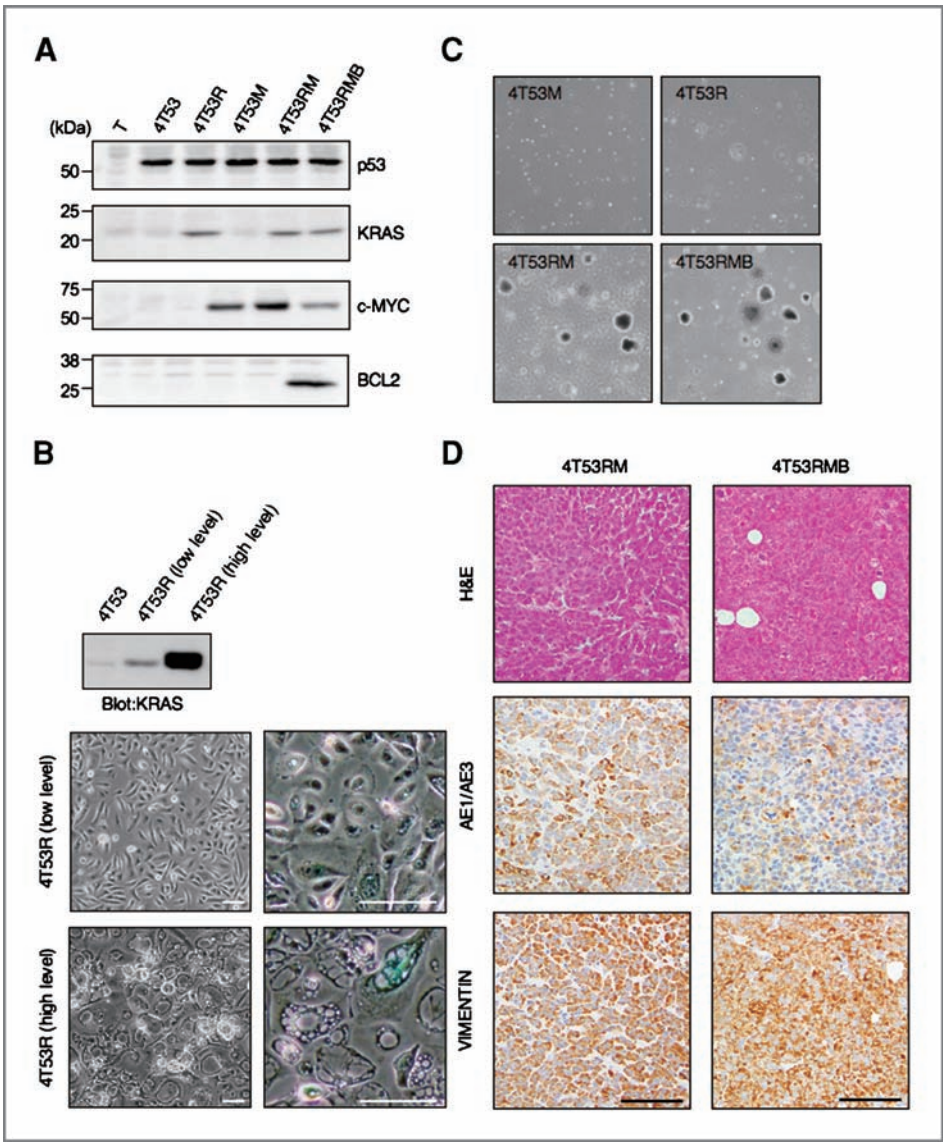

Figure 1. Combined expression of $KRAS^{V12}$ and c-MYC confers tumorigenic potential onto immortalized HSAECs. A, protein extracts (10 μg) from HSAECs infected with retroviral vectors expressing the indicated genes (T, hTERT; 4, CDK4; 53, dominant-negative form of p53; M, c-MYC; R, $KRAS^{V12}$; B, BCL2) were analyzed by immunoblotting. Numbers on left indicate molecular mass (kDa). B, the morphologies (left) and SA-β-gal staining (right) of 4T53 cells expressing high-level (bottom) or low-level $KRAS^{V12}$ (top) are shown. The levels of KRAS protein were confirmed by immunoblotting. Scale bar, 200 μm. C, the anchorage-independent growth properties of 4T53M, 4T53R, 4T53RM, and 4T53RMB cells are shown. D, formalin-fixed, paraffin-embedded tissue sections (4-μm-thick) of xenografts derived from 4T53RM (left) and 4T53RMB (right) cells were subjected to staining for H&E (top), cytokeratins (AE1/AE3; center), and VIMENTIN (bottom). Scale bar, 100 μm.

In an attempt to reproduce well-differentiated lung cancer phenotypes more effectively, we used an active form of PIK3CA (encoding the PI3K catalytic subunit; $PIK3CA^{H1047R}$), CYCLIN-D1, and a dominant-negative form of LKB1 ($LKB1^{D194A}$) instead of c-MYC (Fig. 2A). Mutations and/or overexpression of these factors are associated with non–small-cell lung cancers and with *KRAS* mutations (1). All of the 4T53R-derived cells, expressing $PIK3CA^{H1047R}$ (4T53RP), CYCLIN-D1 (4T53RD), or $LKB1^{D194A}$ (4T53RL), could be propagated as xenografts, although the growth rates varied among the samples (Table 1). We were surprised to discover that the histology of the xenografts obtained from these 4T53R-derived cells accurately recapitulated human lung cancers (Figs. 2 and 3). This is very interesting as flank xenografts derived from cancer cell lines generally have displayed more homogeneous and undifferentiated histologies, indicative of the higher selection pressure occurring *in vitro* during extensive culturing (22).

The 4T53RP xenografts represented human adenosquamous carcinoma containing gland-forming adenocarcinoma-like regions and regions with squamous differentiation (Fig. 2B and 2C), and tumor cells were strongly positive for cytokeratins (AE1/AE3, Fig. 2B; CK8/18, data not shown). Furthermore, p63-staining displayed a unique peripheral staining pattern in 4T53RP xenografts (Fig. 2B), and a similar staining pattern was reported in some adenosquamous carcinomas as well as in the basal reserve cells of normal bronchial epithelium (23). On the other hand, 4T53RD and 4T53RL xenografts comprised of a cytokeratin-positive glandular epithelial malignancy and fibrous stroma (Fig. 2B). Although the 4T53RMB xenografts were totally negative of TTF1-staining, the xenografts showing differentiated histologies contained substantial numbers of tumor cells that were positive for TTF1

Published OnlineFirst March 31, 2011; DOI: 10.1158/0008-5472.CAN-10-2221

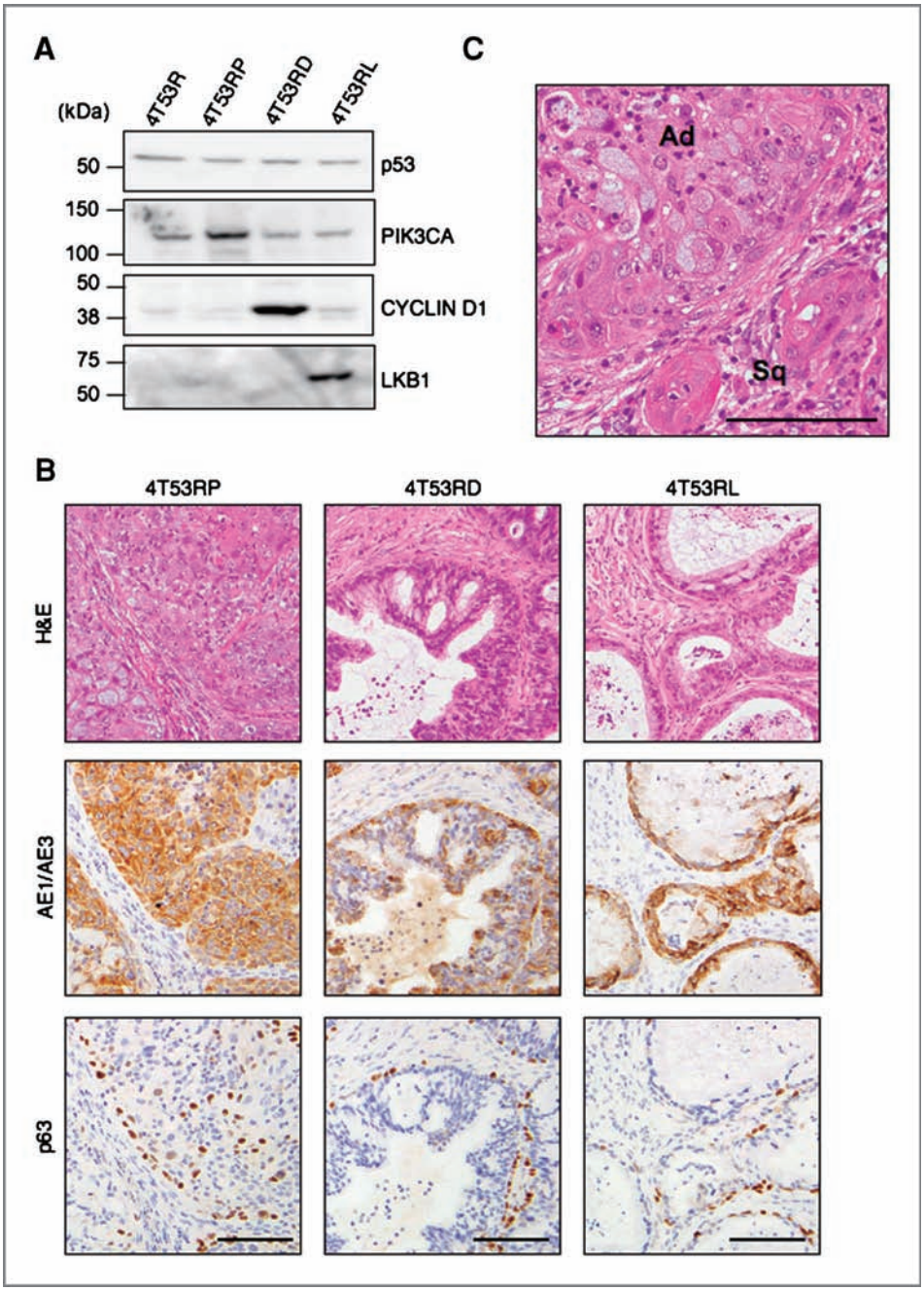

Figure 2. Generation of well-differentiated lung cancer models from immortalized HSAECs. A, protein extracts (10 μg) from 4T53R cells infected with retroviral vectors expressing PIK3CA^{H1047R} (P), CYCLIN-D1 (D) or LKB1^{D194A} (L) were analyzed by immunoblotting. Numbers on left indicate molecular mass (kDa). B, xenograft sections derived from 4T53RP (left), 4T53RD (center), and 4T53RL cells (right) were subjected to H&E staining (top). Immunohistochemical analyses were also carried out using antibodies against cytokeratins (AE1/AE3; center) and p63 (bottom). Scale bar, 100 μm. C, the 4T53RP xenograft contains both adenocarcinoma-like regions (Ad) and regions with squamous differentiation (Sq). Scale bar, 100 μm.

(Fig. 3A), which is frequently expressed in adenocarcinomas and small-cell lung carcinomas (24, 25). Extracellular and intracellular mucin production in differentiated cancers was highlighted by alcian blue staining (Fig. 3B). On the basis of the histological appearance and expression of these markers, we concluded that both 4T53RD and 4T53RL xenografts represented human lung adenocarcinomas with different amounts of stroma (Fig. 2B). Furthermore, reproduction of papillary-subtype phenotypes was especially noted in the 4T53RD xenografts whereas an adenocarcinoma-like region showing an acinar-subtype was detected both in 4T53RD and 4T53RL xenografts. These findings are reasonable because an increased *CYCLIN-D1* gene copy number has been reported in several human cancers including lung adenocarcinomas (26, 27) and *LKB1* mutations, detected in 34% of adenocarcinomas (28), are often associated with *KRAS* mutations (29).

We also made an interesting observation that p63-positive cells were detected in all xenografts displaying differentiated cancer histology (Fig. 2B). This is reasonable, as p63 expression is detectable in all types of lung cancers although its expression is often associated with squamous cell carcinoma

Published OnlineFirst March 31, 2011; DOI: 10.1158/0008-5472.CAN-10-2221

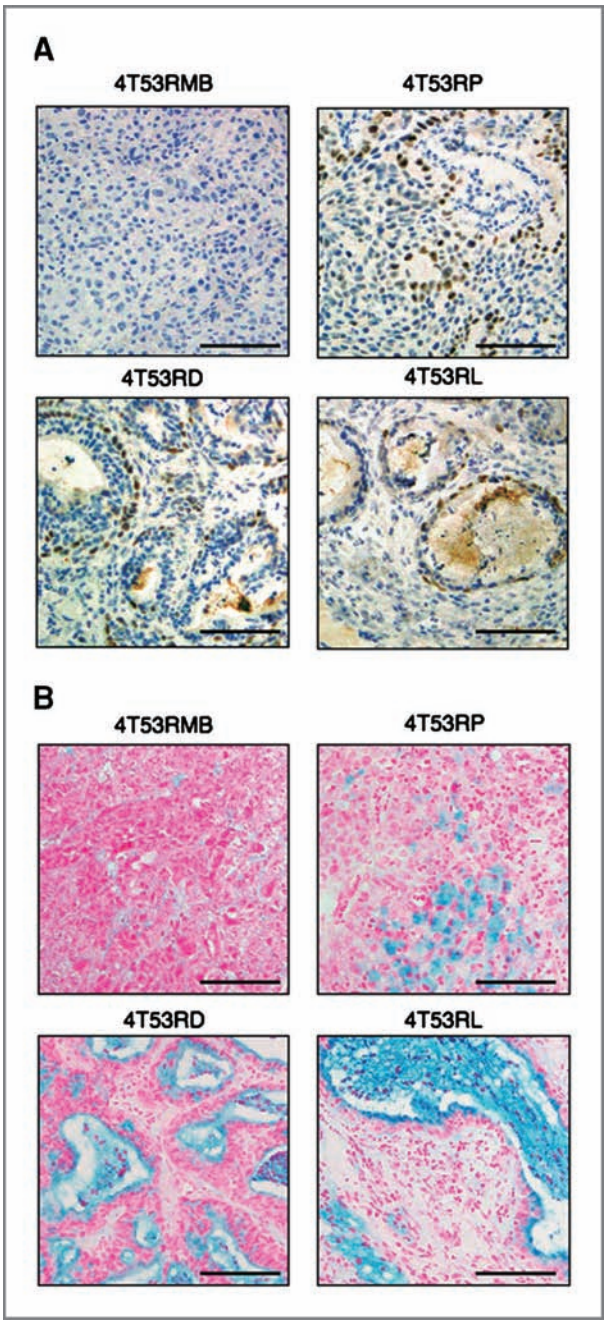

Figure 3. The xenografts with differential histology express adenocarcinoma marker. A, TTF1-positivity of differentiated lung cancer models (4T53RP, 4T53RD, 4T53RL xenografts) were compared with the 4T53RMB xenograft. Scale bar, 100 μm. B, representative images of alcian blue staining of 4T53RMB, 4T53RP, 4T53RD, and 4T53RL xenografts are shown. Scale bar, 100 μm.

(24). However, it should be noted that, particularly in the 4T53RD xenografts, the majority of cytokeratin-positive cancer cells were p63-negative (Fig. 2B) whereas all of 4T53 cells as well as 4T53RD cells expressed p63 in adherent culture (Supplementary Fig. S4A and S4B). As p63-positive basal cells have been identified as stem cells in mouse trachea and human airway epithelium (30), it would be interesting to further characterize the p63-positive and -negative tumor cells in the xenograft specimens.

As the inactivated p53 protein accumulated in 4T53-derived cells (see Fig. 1A), p53-staining allowed us to easily identify tumor cells in stroma-containing xenograft specimens: p53-positive tumor cells are clearly distinguishable from stromal regions in xenografts representing differentiated lung cancers (Fig. 4A). On the other hand, p53- and VIMENTIN-staining almost merged in 4T53RMB xenografts (Fig. 4A), indicating that tumor cells express mesenchymal markers in poorly differentiated cancers. These observations suggest that the epithelial-to-mesenchymal transition (EMT) may particularly occur in xenografts demonstrating poorly differentiated histology. To further investigate the alterations in the morphologies of tumor cells during xenograft propagation, single-cell suspensions obtained from xenografts were cultured under conditions identical to those used for regular HSAEC culture. Primary cultured cells were selected with puromycin, resulting in bulk populations of postgrafted *KRAS*-transformed HSAECs (the KRAS expression plasmid contains the puromycin resistance gene; see Supplementary Fig. S1A). Fibroblastic cells with an elongated shape were predominantly detected in postgrafted 4T53RMB cells whereas pregrafted 4T53RMB cultures displayed a polygonal or round appearance (Fig. 4B). In contrast, postgrafted 4T53RP and 4T53RD cultures displayed an epithelial morphology that was similar to pregrafted matched materials (Fig. 4B). Because one of the hallmarks of EMT is the functional loss of E-CADHERIN (31), we further investigated E-CADHERIN expression. As a result, we found that E-CADHERIN expression was decreased and N-CADHERIN was upregulated in 4T53RMB cells after xenograft propagation, but these changes were not observed in 4T53RP, 4T53RD, or 4T53RL cells (Fig. 4C). Furthermore, p63 expression levels were lower even in pregrafted 4T53RMB cells and they were lost in postgrafted cells, whereas *KRAS*-transformed HSAEC lines other than 4T53RMB cells clearly maintained p63 expression (Fig. 4C).

Discussion

In mouse models of human cancers, including lung cancer, tumors spontaneously arise and recapitulate the histologic, spatial, and temporal context of the corresponding human diseases, and these models have proven to be valuable tools not only for understanding the basic cancer biology but also for proof-of-concept studies of molecular targeted therapies (1, 32). However, genetic models are often not suited to high-throughput studies for potential new treatments as this approach is usually time-consuming and labor-intensive. Furthermore, fundamental differences in the biology between human and rodent cells have been demonstrated (3, 4), and therefore, it has been important to complement studies on genetic models with approaches involving human cancer cells propagated *in vitro* and *in vivo*. The majority of preclinical cancer studies have employed xenograft models established from human tumor cell lines in the flank of

Published OnlineFirst March 31, 2011; DOI: 10.1158/0008-5472.CAN-10-2221

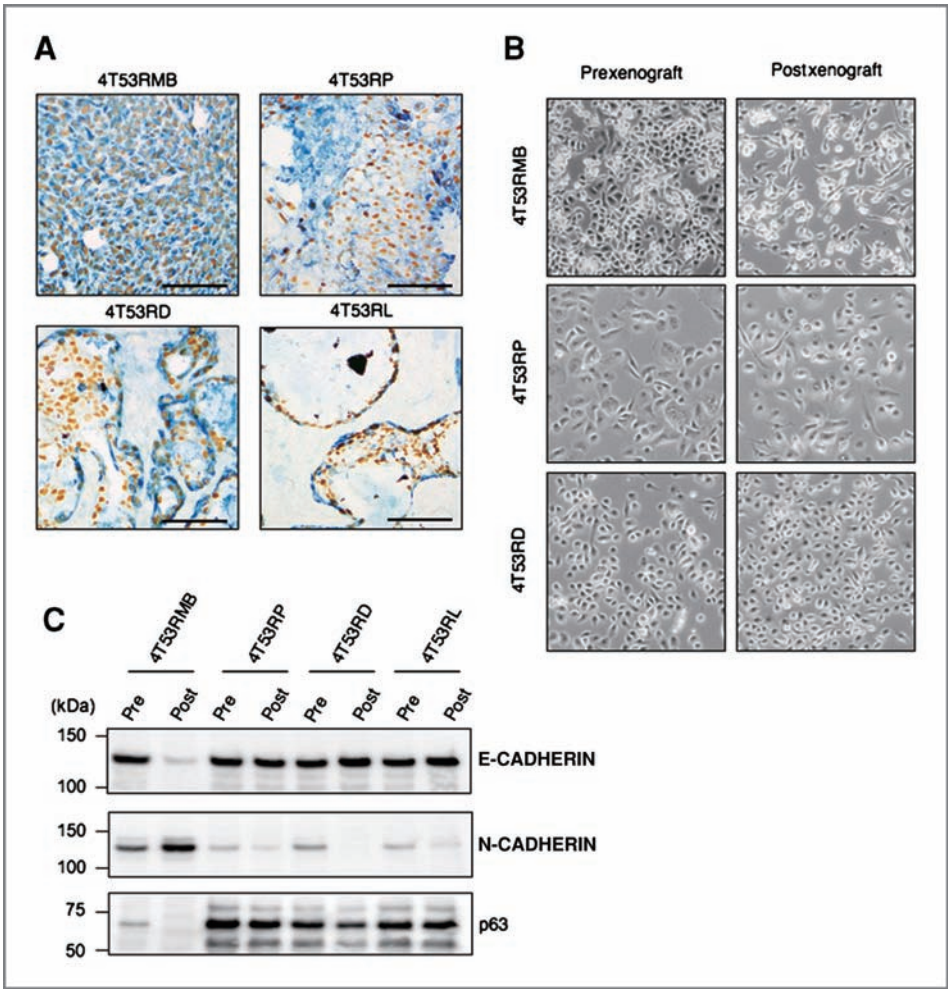

Figure 4. EMT occurs in poorly differentiated cancers but not in well-differentiated cancers during xenograft propagation. A, double staining of HSAEC-derived xenografts was carried out using anti-p53 (brown) and anti-VIMENTIN antibodies (blue). Scale bar, 100 μm. B, single cell suspensions were isolated from 4T53RMB, 4T53RP, and 4T53RD xenografts and maintained in SAGM medium. Their morphologies (right, postxenograft) were compared with pregrafted matched materials (left, prexenograft). C, protein extracts (10 μg) from 4T53-derived cultures of pre- and postxenograft propagation experiments were analyzed by immunoblotting. Numbers on left indicate molecular mass (kDa).

immunocompromised mice (22). Although these models are often assumed to be representative of the original disease, it is unclear to what degree such experimental models replicate the phenotype of the original human cancers as the tumor cells have been removed from their native environment and selected for their ability to grow under artificial conditions. In addition, cancer cell lines often harbor a large number of undefined genetic lesions which complicates the study of specific molecules and pathways. These considerations raise concerns about many of the human tumor xenografts that are currently being used to test anticancer drugs. In fact, a recent study has proposed that genetically engineered mouse models can improve the ability to predict patient outcomes in clinical trials compared with the xenografts derived from cancer cell lines (33).

Here we have succeeded in immortalizing HSAECs by introducing genes for multiple cellular factors and further converting these immortalized cells (4T53 cells) into malignant cells by additionally expressing c-MYC, PIK3CA^{H1047R}, CYCLIN-D1, or LKB1^{D194A} in combination with KRAS^{V12}. As growth rates were almost indistinguishable between all of the transformed cells in adherent culture, and were slightly higher than those of immortalized cells, differences in the growth properties among transformed HSAECs were particularly evident after transplantation. The cytogenetic analyses indicated that both immortalized and transformed cells were nearly diploid, whereas approximately 10% of 4T53RMB cells were tetraploid (Supplementary Fig. S2B and 2C). We also found that substantial numbers of 4T53RP, 4T53RD, and 4T53RL cells were trisomic for chromosomes 11 and 20 (Supplementary Fig. S2B), consistent with the previous observation that the duplication of chromosome 20 was frequently observed in immortalized human bronchial epithelial cells (6). However, the trisomy for chromosome 20 was rarely seen in the 4T53 cells as well as in 4T53RMB cells (Supplementary Fig. S2B). Therefore, it is possible that gain of chromosome 20 might not necessarily be required for cellular immortalization or transformation in the case of HSAECs.

We confirmed the tumorigenic effects of these combinations of oncogenes by employing another independent batch of HSAECs derived from an individual with a different age, gender, and race (HSAEC-2; from a 47-year-old Hispanic male). Although tumor incidence, latency and histology of 4T53RMB cells were similar between the 2 types of HSAECs, larger

Published OnlineFirst March 31, 2011; DOI: 10.1158/0008-5472.CAN-10-2221

numbers of cells and longer latency were required to obtain differentiated lung cancers in the case of HSAEC-2 (Supplementary Fig. S5A). Similar to the case of the first line, xenografts derived from the HSAEC-2_4T53RD cells represented lung adenocarcinomas (Supplementary Fig. S5A and S5B). However, histological features of the 4T53RP-derived xenograft were moderately different between HSAEC and HSAEC-2. The xenografts derived from HSAEC-2_4T53RP cells represented human lung squamous-cell carcinoma: gland-forming adenocarcinoma-like regions were rarely observed whereas they were frequently detected in the case of the first line (Supplementary Fig. S5A and S5B). These observations are consistent with a previous report showing that mutation or amplification of *PIK3CA* was found in a subgroup of non–small-cell lung cancers and squamous-cell carcinomas in particular (34). The difference in the histology between 2 independent batches of HSAECs might depend on the different origins of the cells. It is possible that HSAEC-2 might contain cells that were isolated from the more proximal region of the lung. As human lung squamous-cell carcinoma usually arises in the proximal lung, it would be interesting to test whether transformed bronchial epithelial cells effectively reproduce squamous-cell carcinoma phenotypes. Collectively, we concluded that immortalized HSAECs can be converted into cancer cells when $KRAS^{V12}$ is introduced in combination with an additional cellular oncogene as described previously.

The most important observation made here is that several HSAEC-derived flank xenografts (4T53RP, 4T53RD, and 4T53RL) reproduce the human lung adenocarcinoma phenotype. This is a surprising finding as the adenocarcinoma phenotype is difficult to recapitulate in xenograft models. In fact, although differentiated breast cancers have been generated by the propagation of transformed mammary/breast epithelial cells in the mammary fat pad (35), the generation of differentiated cancer models from normal human epithelial cells has rarely been successful. As adenocarcinoma constitutes a large majority of lung cancers (1, 2), the present flank xenograft models offer a convenient system for high-throughput studies of potential new therapies. In addition to differentiated lung cancer models, poorly differentiated cancer models can also be engineered, indicating that the histological features and degree of differentiation are controllable to some extent by changing the combination of genetic elements introduced. The degree of differentiation of human tumors is routinely assessed in the clinic, with poorly differentiated tumors generally having the worst prognosis. As the exploration of factors that are present in poorly differentiated cancers but are absent in well-differentiated cancers should reveal potential molecular targets, our model system is useful to find and authenticate molecules with promise for therapeutic targeting.

One of the greatest benefits of our system may be its applications for high-throughput screening systems. There has been increasing hope that novel molecular targeted therapies will be efficacious in the treatment of specific tumors and cell line–based screening for anticancer drugs has been carried out for several decades. However, such screening strategies have often been hampered by the lack of "appropriate counterparts", because many cytotoxic compounds are toxic to cancer cells as well as all other proliferating cells. Conversely, our system allows us to propagate both normal/immortalized and tumorigenic cells under the same conditions *in vitro*. Thus, the use of isogenic cells (i.e., normal/immortalized versus transformed samples) should prove to be a powerful tool for high-throughput screening. In fact, the use of experimentally immortalized and transformed mammary epithelial cells has succeeded in identifying selective inhibitors of cancer stem cells using high-throughput screening (36). Collectively, engineered cancer cells derived from normal HSAECs can serve as valuable reagents not only to elucidate the molecular basis of lung cancer development but also to identify candidate targets for anticancer drugs by high-throughput screening, ultimately improving future therapies.

Disclosure of Potential Conflicts of Interest

No potential conflicts of interest were disclosed.

Acknowledgment

We are grateful to Dr Christopher Calabrese (St Jude Children's Research Hospital, Memphis, TN, USA) for critical reading of this manuscript.

The costs of publication of this article were defrayed in part by the payment of page charges. This article must therefore be hereby marked *advertisement* in accordance with 18 U.S.C. Section 1734 solely to indicate this fact.

Received June 22, 2010; revised November 26, 2010; accepted January 30, 2011; published online March 29, 2011.

References

1. Meuwissen R, Berns A. Mouse models for human lung cancer. Genes Dev 2005;19: 643–64.
2. Herbst RS, Heymach JV, Lippman SM. Lung cancer. N Engl J Med 2008;359:1367–80.
3. Akagi T. Oncogenic transformation of human cells: shortcomings of rodent model systems. Trends Mol Med 2004;10:542–8.
4. Zhao JJ, Roberts TM, Hahn WC. Functional genetics and experimental models of human cancer. Trends Mol Med 2004;10:344–50.
5. Sato M, Vaughan MB, Girard L, Peyton M, Lee W, Shames DS, et al. Multiple oncogenic changes (K-RAS(V12), p53 knockdown, mutant EGFRs, p16 bypass, telomerase) are not sufficient to confer a full malignant phenotype on human bronchial epithelial cells. Cancer Res 2006;66:2116–28.
6. Ramirez RD, Sheridan S, Girard L, Sato M, Kim Y, Pollack J, et al. Immortalization of human bronchial epithelial cells in the absence of viral oncoproteins. Cancer Res 2004;64:9027–34.
7. Lundberg AS, Randell SH, Stewart SA, Elenbaas B, Hartwell KA, Brooks MW, et al. Immortalization and transformation of primary human airway epithelial cells by gene transfer. Oncogene 2002;21:4577–86.
8. Sekido Y, Fong KM, Minna JD. Molecular genetics of lung cancer. Annu Rev Med 2003;54:73–87.
9. Saenz-Robles MT, Sullivan CS, Pipas JM. Transforming functions of Simian Virus 40. Oncogene 2001;20:7899–907.
10. Cheng J, DeCaprio JA, Fluck MM, Schaffhausen BS. Cellular transformation by Simian Virus 40 and Murine Polyoma Virus T antigens. Semin Cancer Biol 2009;19:218–28.

Published OnlineFirst March 31, 2011; DOI: 10.1158/0008-5472.CAN-10-2221

11. Akagi T, Sasai K, Hanafusa H. Refractory nature of normal human diploid fibroblasts with respect to oncogene-mediated transformation. Proc Natl Acad Sci U S A 2003;100:13567–72.
12. Sasai K, Romer JT, Lee Y, Finkelstein D, Fuller C, McKinnon PJ, et al. Shh pathway activity is down-regulated in cultured medulloblastoma cells: implications for preclinical studies. Cancer Res 2006;66:4215–22.
13. Sasai K, Nodagashira M, Nishihara H, Aoyanagi E, Wang L, Katoh M, et al. Careful exclusion of non-neoplastic brain components is required for an appropriate evaluation of O6-methylguanine-DNA methyltransferase status in glioma: relationship between immunohistochemistry and methylation analysis. Am J Surg Pathol 2008;32:1220–7.
14. Akagi T, Murata K, Shishido T, Hanafusa H. v-Crk activates the phosphoinositide 3-kinase/AKT pathway by utilizing focal adhesion kinase and H-Ras. Mol Cell Biol 2002;22:7015–23.
15. Shaulian E, Zauberman A, Ginsberg D, Oren M. Identification of a minimal transforming domain of p53: negative dominance through abrogation of sequence-specific DNA binding. Mol Cell Biol 1992;12:5581–92.
16. Drane P, Leblanc V, Miro-Mur F, Saffroy R, Debuire B, May E. Accumulation of an inactive form of p53 protein in cells treated with TNF alpha. Cell Death Differ 2002;9:527–37.
17. Heyne K, Schmitt K, Mueller D, Armbruester V, Mestres P, Roemer K. Resistance of mitochondrial p53 to dominant inhibition. Mol Cancer 2008;7:54.
18. Sasaki R, Narisawa-Saito M, Yugawa T, Fujita M, Tashiro H, Katabuchi H, et al. Oncogenic transformation of human ovarian surface epithelial cells with defined cellular oncogenes. Carcinogenesis 2009;30:423–31.
19. Eilers M, Eisenman RN. Myc's broad reach. Genes Dev 2008;22:2755–66.
20. Wong DJ, Liu H, Ridky TW, Cassarino D, Segal E, Chang HY. Module map of stem cell genes guides creation of epithelial cancer stem cells. Cell Stem Cell 2008;2:333–44.
21. Schoenhals M, Kassambara A, De Vos J, Hose D, Moreaux J, Klein B. Embryonic stem cell markers expression in cancers. Biochem Biophys Res Commun 2009;383:157–62.
22. Kelland LR. Of mice and men: values and liabilities of the athymic nude mouse model in anticancer drug development. Eur J Cancer 2004;40:827–36.
23. Wang BY, Gil J, Kaufman D, Gan L, Kohtz DS, Burstein DE. P63 in pulmonary epithelium, pulmonary squamous neoplasms, and other pulmonary tumors. Hum Pathol 2002;33:921–6.
24. Borczuk AC, Gorenstein L, Walter KL, Assaad AA, Wang L, Powell CA. Non-small-cell lung cancer molecular signatures recapitulate lung developmental pathways. Am J Pathol 2003;163:1949–60.
25. Nakamura N, Miyagi E, Murata S, Kawaoi A, Katoh R. Expression of thyroid transcription factor-1 in normal and neoplastic lung tissues. Mod Pathol 2002;15:1058–67.
26. Gautschi O, Ratschiller D, Gugger M, Betticher DC, Heighway J. Cyclin D1 in non-small cell lung cancer: a key driver of malignant transformation. Lung Cancer 2007;55:1–14.
27. Betticher DC, Heighway J, Hasleton PS, Altermatt HJ, Ryder WD, Cerny T, et al. Prognostic significance of CCND1 (cyclin D1) overexpression in primary resected non-small-cell lung cancer. Br J Cancer 1996;73:294–300.
28. Ji H, Ramsey MR, Hayes DN, Fan C, McNamara K, Kozlowski P, et al. LKB1 modulates lung cancer differentiation and metastasis. Nature 2007;448:807–10.
29. Koivunen JP, Kim J, Lee J, Rogers AM, Park JO, Zhao X, et al. Mutations in the LKB1 tumour suppressor are frequently detected in tumours from Caucasian but not Asian lung cancer patients. Br J Cancer 2008;99:245–52.
30. Rock JR, Onaitis MW, Rawlins EL, Lu Y, Clark CP, Xue Y, et al. Basal cells as stem cells of the mouse trachea and human airway epithelium. Proc Natl Acad Sci U S A 2009;106:12771–5.
31. Peinado H, Olmeda D, Cano A. Snail, Zeb and bHLH factors in tumour progression: an alliance against the epithelial phenotype?Nat Rev Cancer 2007;7:415–28.
32. Tuveson DA, Jacks T. Modeling human lung cancer in mice: similarities and shortcomings. Oncogene 1999;18:5318–24.
33. Singh M, Lima A, Molina R, Hamilton P, Clermont AC, Devasthali V, et al. Assessing therapeutic responses in Kras mutant cancers using genetically engineered mouse models. Nat Biotechnol 2010;28:585–93.
34. Yamamoto H, Shigematsu H, Nomura M, Lockwood WW, Sato M, Okumura N, et al. PIK3CA mutations and copy number gains in human lung cancers. Cancer Res 2008;68:6913–21.
35. Ince TA, Richardson AL, Bell GW, Saitoh M, Godar S, Karnoub AE, et al. Transformation of different human breast epithelial cell types leads to distinct tumor phenotypes. Cancer Cell 2007;12:160–70.
36. Gupta PB, Onder TT, Jiang G, Tao K, Kuperwasser C, Weinberg RA, et al. Identification of selective inhibitors of cancer stem cells by high-throughput screening. Cell 2009;138:645–59.

Cancer Research
The Journal of Cancer Research (1916–1930) | The American Journal of Cancer (1931–1940)

AACR American Association for Cancer Research

Oncogene-Mediated Human Lung Epithelial Cell Transformation Produces Adenocarcinoma Phenotypes *In Vivo*

Ken Sasai, Taiko Sukezane, Emmy Yanagita, et al.

Cancer Res 2011;71:2541-2549. Published OnlineFirst March 31, 2011.